AIAA Guidance, Navigation, and Control Conference
13 - 16 August 2012, Minneapolis, Minnesota

AIAA 2012-4826

Optimal Trajectory and Control Generation for Landing of Multiple Aircraft in the Presence of Obstacles

Krithika Mohan*
Michael A. Patterson†
Anil V. Rao‡

University of Florida
Gainesville, FL 32611

I. Introduction

Due to the large increase in the density of aircraft arrivals at airports in recent years, it has become important to optimize the scheduling of aircraft landings in order to reduce wait time, improve airport efficiency, and minimize fuel consumption while maintaining safety. As the density of aircraft arrivals increases, however, so too does the complexity of trajectory planning and generation. A key aspect of landing multiple aircraft on a single runway is conflict detection and resolution. In the context aircraft landing, a conflict is defined as the situation of loss of minimum safe separation between two aircraft Ref. 1. The conflict detection and resolution process consists of predicting, communicating to the pilot, and resolving the conflict. Typically, evaluating the likelihood of a conflict is based on the current position and velocity of an aircraft. The conflict is then resolved by determining a maneuver required by one or more aircraft to avoid the predicted conflict. The required information is then provided to the air traffic controller who communicates with the pilot to resolve the conflict.

A great deal of research has been done on the problem of multiple-aircraft conflict detection and resolution and landing of multiple aircraft. Ref. 2 considers the problem of managing landing sequences for an arbitrary number of aircraft moving in the vicinity of a controlled aerodome. Ref. 3 considers how different airport landing sequencing algorithms affect both the arrival sequence of aircraft and air traffic control. Ref. 4 develops an approach for determining optimal trajectories to bring an unmanned aerial vehicle from a loitering state to a planted landing. Ref. 5 develops a queueing algorithm for routing aircraft on two airport runways. Ref. 6 considers a three-dimensional trajectory optimization algorithm is developed by to obtain a conflict-free flight path using a nonlinear point mass model with realistic operational constraints on individual aircraft. Ref. 7 considers the problem of optimal cooperative three-dimensional conflict resolution involving multiple aircraft, where the the initial and final locations of the aircraft are specified along with detailed point-mass aircraft dynamic models. The infinite-dimensional optimal control problem is then converted into a finite dimensional nonlinear program (NLP) using collocation on finite elements. Finally, Ref. 8

*MS Student. Department of Mechanical and Aerospace Engineering. E-mail: krithi12@gmail.com.
†Ph.D. Student, Deparment of Mechanical and Aerospace Engineering. E-mail: mpatterson@ufl.edu.
‡Associate Professor. Department of Mechanical and Aerospace Engineering. E-mail: anilvrao@ufl.edu. Corresponding Author. Associate Fellow AIAA.

proposes an autonomous counter-hijack control of aircraft, where the critical buildings are modeled as obstacles to be avoided in the aircraft path.

The previously cited research shows that determining optimal aircraft landing trajectories and controls is important for improving air traffic control efficiency. Abstractly, an optimal multiple-aircraft landing problem can be posed as a constrained nonlinear optimal control problem. In general, such problems do not have analytical solutions and, thus, must be solved numerically. In this Note we develop an approach that uses direct collocation for determining optimal trajectories and controls for multiple aircraft landing on a single runway in the presence of an obstacle, where the obstacle represents a constraint that may occur in an urban environment (e.g., having to pass between two buildings) or in a situation where it is necessary to specify keep-away zones for each of two aircraft landing simultaneously on neighboring runways. In addition to the obstacle constraint, the aircraft are subject to time spacing constraints between successive aircraft landings and collision-avoidance constraints. Furthermore, we develop a hybrid cost functional that keep the aircraft away from the obstacle for as long as possible during pre-obstacle flight and minimizes the amount of control effort across the entire trajectory of each aircraft. The optimal aircraft landing problem is formulated as a constrained multiple-phase optimal control problem and is solved using a two-stage approach. The first stage consists of a rapidly exploring random tree (RRT) algorithm that generates initial guesses for the optimal control solver.[9] The RRT algorithm used in this research generates initial guesses that are feasible with respect to the obstacle constraint and provides a good starting point for numerical optimization. Using the initial guesses generated from the RRT algorithm, the second stage consists of solving the multiple-phase optimal control problem using the *hp*–adaptive[10,11] version of the open-source optimal control software *General Pseudospectral Optimal Control Software*[10–12] (GPOPS). The approach is quite general in that each aircraft can have a different model, making it possible to use the approach of this paper to land different types of aircraft including both horizontal and vertical take-off and landing vehicles. The method developed in this paper is applied to closely-spaced two-, three-, and four–aircraft landing scenarios and the key features of the optimal trajectories are identified.

It is noted that Ref. 13 also considers a two-stage path planning approach for designing multiple spacecraft reconfiguration maneuvers. In Ref. 13, a bi-directional RRT path planning algorithm is utilized to quickly provide a feasible initial guess, but without considering the differential equation constraints. A transition algorithm then augments the guess from the RRT algorithm with another guess where the dynamics are propagated from the initial time to the terminal time. This new guess is then used as an input to solving the optimal control problem using the Gauss pseudospectral method.[14,15] While this paper utilizes some of the concepts utilized in Ref. 13, the problem of interest is quite different in that Ref. 13 considers a problem where the phases are sequential and the motion of the vehicles occurs simultaneously while in this paper we consider a problem with non-sequential and only partially overlapping phases. In addition, in this paper we incorporate both collision-avoidance and obstacle-avoidance constraints along with interior-point constraints that enable the vehicle to safely pass through an opening in the obstacle.

This paper is organized as follows. In Section II, the multiple aircraft landing problem is formulated along with the equations of motion of the aircraft and the controls. Also the method for obstacle formulation in three-dimension is described. In Section III, the optimal multiple-aircraft landing problem is described. In Section IV the rapidly exploring random tree algorithm for generating initial guesses is described. In Section V results of solving the non-sequential multiple-phase optimal control problem of Section III are provided for two, three, and four aircraft. Finally, in Section VI we provide conclusions of our work.

II. Problem Formulation

Consider a total of A aircraft flying in the vicinity of a single airport runway. The goal is to land the aircraft safely on the runway while placing time constraints on the time between aircraft landings, collision-avoidance path constraints, and obstacle-avoidance constraints, while optimizing a specified performance index. The performance index used in this paper is a combination of maximizing the time taken by each aircraft to pass through an opening in the obstacle and minimizing the crossrange maneuvering performed by each aircraft across the entire trajectory. In this section we formulate the problem under consideration in this Note.

A. Equations of Motion and Vehicle Model

The equations of motion A aircraft moving at constant speed V over a flat Earth are given as

$$\begin{aligned} &\dot{x}_i(t) = V\cos\gamma_i(t)\cos\phi_i(t) \quad , \quad \dot{y}_i(t) = V\cos\gamma_i(t)\sin\phi_i(t), \\ &\dot{h}_i(t) = V\sin\gamma_i(t) \quad , \quad \dot{\gamma}_i(t) = \frac{g}{V}\left[n_{vi}(t) - \cos\gamma_i(t)\right], \quad i = 1,\ldots,A, \\ &\dot{\phi}_i(t) = \frac{g}{V}\frac{n_{hi}(t)}{\cos\gamma_i(t)}, \end{aligned} \tag{1}$$

where $x_i(t)$ and $y_i(t)$ are the horizontal Cartesian components of position, $h_i(t)$ is the vertical Cartesian component of position (that is, the altitude), $\gamma_i(t)$ is the flight path angle, and $\phi_i(t)$ is the heading angle of aircraft $i \in [1,\ldots,A]$. Furthermore, $n_{hi}(t)$ and $n_{vi}(t)$ are, respectively, the horizontal and vertical components of the load factor of aircraft $i \in [1,\ldots,A]$ (and are the two controls in this problem). The total load factor and the bank angle of aircraft $i \in [1,\ldots,A]$ are then computed, respectively, as

$$n_i(t) = \sqrt{n_{hi}^2(t) + n_{vi}^2(t)} \text{ and } \sigma_i(t) = \tan^{-1}\left(n_{hi}(t), n_{vi}(t)\right), \tag{2}$$

where $\tan^{-1}(\cdot,\cdot)$ is the four-quadrant inverse tangent function. For compactness later in the discussion we will often refer to the state as $\mathbf{p}(t) = (x(t), y(t), h(t), \gamma(t), \phi(t))$. Finally, it is noted that in the region of interest in this paper the speed does not vary significantly and, thus, the assumption that the aircraft move with constant speed is reasonable.

B. Trajectory Event Sequence

The total trajectory design is divided into $2A$ partially overlapping phases. Phases $j \in [1,\ldots,A]$ start with each of the aircraft that remain in the airspace and have not passed through the opening in the obstacle wall, and terminate with the aircraft that was closest to the runway at the start of phase j passing through the opening in the wall obstacle. Phases $j + A \in [A+1,\ldots,2A]$ start with the aircraft that passed through the opening in the wall obstacle in phase $j \in [1,\ldots,A]$ and terminates with this same aircraft landing on the runway. Furthermore, phases $j \in [1,\ldots,A]$ consist of $n = A - j + 1$ aircraft flying towards the obstacle wall, while phases $j + A \in [A+1,\ldots,2A]$ consist of only a single aircraft that is on its way to landing on the runway. Finally, it is noted that t_j^o denotes the time at which the aircraft that is closest in distance to the obstacle at the start of phase $j \in [1,\ldots,A]$ must pass through the opening in the wall obstacle, while t_{fj} denotes the time that this same aircraft lands on the runway.

C. Boundary, Event, State-Continuity, and Path Constraints

The initial and terminal conditions of each aircraft are given, respectively, as $\mathbf{p}(t_0) = \mathbf{p}_0$ and $\mathbf{p}(t_{fi}) = \mathbf{p}_f,\ i = 1,\ldots,A$, where t_0 is the initial time and t_{fi} is the landing time of aircraft $i \in [1,\ldots,A]$.

It is noted that each of the landing times, $t_{fi},\ i = 1,\ldots,A$, are fixed, and the final state, $\mathbf{p}_f = (x_f, y_f, h_f, \gamma_f, \phi_f)$, is the same for each aircraft. In terms of t_{fj}, the final landing times for each of the aircraft are given as $t_{fj} = t_{f,j-1} + T, \quad j \in [2,\ldots,A]$, where T defines the time difference between aircraft landing times.

Next, event constraints are enforced at the ends of phases $j \in [1,\ldots,A]$. These constraints ensure that each aircraft passes through the opening in the obstacle wall such that the velocity of the aircraft is parallel to the ground. First, to ensure that the aircraft closest in distance to the obstacle at the start of phase $j \in [1,\ldots,A]$ passes through the opening in the obstacle while staying within the boundaries of the opening in the obstacle, the following constraints are imposed at $t_j^o,\ j = 1,\ldots,A$]: $-x^o_{\max} \le x(t_j^o) \le x^o_{\max},\ y(t_j^o) = y^o,\ h^o_{\min} \le h(t_j^o) \le h^o_{\max},\ j = 1,\ldots,A$, where $\pm x^o_{\max}$, $h^o_{\min}$, and $h^o_{\max}$ define the size and location of the opening in the obstacle, and y^o defines the location of the plane of the obstacle. It is also required that each aircraft pass through the opening in the obstacle such that its velocity is parallel to the ground and orthogonal to the plane of the obstacle. The constraints at the point where an aircraft must pass through the opening in the obstacle are then given as $\gamma(t_j^o) = 0$ and $\phi(t_j^o) = \phi^o, \quad j = 1,\ldots,A$, where ϕ^o is the value of the heading angle that corresponds to the aircraft heading in a direction that is orthogonal to the plane of the obstacle at the point where the aircraft must pass through the opening in the obstacle.

Next, in order for the trajectory to be continuous across phases, the following continuity constraints are enforced at the phase boundaries. First, between phases $j \in [1,\ldots,A-1]$ and $j+1 \in [2,\ldots,A]$, continuity on the state and time of each aircraft that have not yet passed through the opening in the obstacle is enforced via the linkage constraints $\mathbf{p}_i(t_f^{(j)}) = \mathbf{p}_i(t_0^{(j+1)})$ and $t_f^{(j)} = t_0^{(j+1)},\ j = 1,\ldots,A-1, \quad i = j+1,\ldots,n$, where $t_f^{(j)}$ are the final times of phases $j \in [1,\ldots,A-1]$, $t_0^{(j+1)}$ are the initial time of phases $j+1 \in [2,\ldots,A]$, and $n = A - j + 1$ is the number of aircraft in phase $j \in [1,\ldots,A-1]$. Next, continuity in the state and time of the n aircraft between phases $j \in [1,\ldots,A]$ and $j + A \in [A+1,\ldots,2A]$ is enforced as $\mathbf{p}_k(t_f^{(j)}) = \mathbf{p}_k(t_0^{(j+A)})$ and $t_{fk}^{(j)} = t_{0k}^{(j+A)},\ j = 1,\ldots,A$, where the subscript k corresponds to the aircraft that was closest in distance to the obstacle at the start of phase $j \in [1,\ldots,A]$, and, consequently, corresponds to the aircraft that is landing in phase $j + A \in [A+1,\ldots,2A]$.

Next, the following path constraints are enforced during the trajectory. First, the state is box-constrained as $\mathbf{p}_{\min} \le \mathbf{p}(t) \le \mathbf{p}_{\max},\ i = 1,\ldots,A$, where the first three components of $\mathbf{p}_{\min}$ and $\mathbf{p}_{\max}$ define the allowable limits on the three-dimensional airspace while the fourth and fifth components on $\mathbf{p}_{\min}$ and $\mathbf{p}_{\max}$ define the constraints on the allowable directions of velocity. Next, it is assumed in this paper that during flight each aircraft must pass through an opening in a rectangular obstacle. The opening is constructed by superimposing four rectangular walls, where each wall has its own size and center point. Because a rectangle is a non-differentiable function, it is replaced with the following differentiable approximation placed at a plane located at $y = y_h$:

$$q_k(x,h) = \left(\frac{x - x_{ck}}{a_k}\right)^p + \left(\frac{h - h_{ck}}{c_k}\right)^p = d_k^p, \quad (k = 1,\ldots,4), \tag{3}$$

where a_k and c_k, $k \in [1,\ldots,4]$, represent the lengths of the walls in the x and h directions, d_k, $k \in [1,\ldots,4]$, is the radius of the wall, x_{ck} and h_{ck}, $k \in [1,\ldots,4]$, are the x and h coordinates of the position of the center points of the walls, and p is an even positive integer. In order for each aircraft to pass through the opening formed by the composition of the four walls, it is necessary that $q_k(x(t), h(t)) > d_k^p, \quad (k = 1,\ldots,4)$. In order to increase computational tractability, q_k is replaced with its natural logarithm as $O_k = \ln q_k > p \ln d_k, \quad (k = 1,\ldots,4)$.

In addition to the requirement that each aircraft pass through an opening in the obstacle, it is also necessary that the aircraft not collide during flight. Because only pre-obstacle phases $i \in [1,\ldots,A-1]$ contain multiple aircraft (and, thus, are the only phases where collision can

occur), collision-avoidance path constraints are only enforced in phases $i \in [1, \ldots, A-1]$. The collision avoidance constraints are formulated as follows. Let (x_a, y_a, h_a) and (x_b, y_b, h_b) be the Cartesian positions of two distinct aircraft a and b (that is, $a \neq b$) in phase $i \in [1, \ldots, A-1]$. Then the number of collision avoidance constraints in phase $i \in [1, \ldots, A-1]$ will be $n(n-1)/2$, where $n = A - i + 1$ is the number of aircraft remaining in the airspace in phase i. The collision avoidance constraints in phase $i \in [1, \ldots, A-1]$ are then given as

$$(x_a(t) - x_b(t))^2 + (y_a(t) - y_b(t))^2 + (h_a(t) - h_b(t))^2 \geq \ell^2, \quad \begin{array}{l} a = 1, \ldots, n, \\ b = a+1, \ldots, n, \\ a \neq b, \end{array} \tag{4}$$

where ℓ is a parameter that corresponds to a safe separation distance.

In addition to the aforementioned path constraints, the following control constraints are applied to each vehicle during flight. First, each control, n_h and n_v, are constrained as $-n_{\max} \leq n_{hi}(t) \leq n_{\max}$ and $-n_{\max} \leq n_{vi}(t) \leq n_{\max},\ i = 1, \ldots, A$, where the value for $n_{\max}$ used in this paper is taken from Ref. 16 (see Section V). Next, the total load factor on each aircraft is constrained as $n_{hi}^2(t) + n_{vi}^2(t) \leq n_{\max}^2,\quad i = 1, \ldots, A$. Finally, in order to limit the amount of crossrange maneuvering that each aircraft is capable of performing, the following constraint is imposed on the bank angle of each aircraft throughout the trajectory: $-\sigma_{\max} \leq \sigma_i(t) \leq \sigma_{\max},\ i = 1, \ldots, A$.

D. Cost Functional

In this problem, the cost functional is a combination of maximizing the time required for each aircraft to reach the opening in the obstacle and minimizing the control effort of each vehicle over the entire duration of the flight. First the time taken by any aircraft $i \in [1, \ldots, A]$ to reach the opening in the obstacle is given as

$$\Phi_i = t_i^o, \quad i = 1, \ldots, A. \tag{5}$$

Next, the cost associated for steering performed by each of the n aircraft in phase j is given as

$$L_{jk} = \int_{t_0}^{t_f} \left(\dot{\gamma}_{jk}^2(t) + \dot{\phi}_{jk}^2(t) \right) dt, \quad (j = 1, \ldots, 2A), \quad (k = 1, \ldots, n), \tag{6}$$

The cumulative cost functional is then given as

$$J = -c \sum_{i=1}^{A} \Phi_i + \sum_{j=1}^{2A} \sum_{k=1}^{n} L_{jk}, \tag{7}$$

where c is a positive scale factor. It is noted that the Mayer cost attempts to increase the time for each aircraft to reach the obstacle while the Lagrange cost attempts to reduce control actuation because $\dot{\gamma}$ and $\dot{\phi}$ are functions of the two components of control, n_h and n_v.

III. Optimal Control Problem

The multiple-aircraft landing optimal control problem described is now stated as follows. Determine the trajectories of each of the A aircraft that minimize the cost functional of Eq. (7) subject to the dynamic constraints of Eq. (1) and the boundary conditions, event constraints, and path constraints given in Section C. The optimal control problem is solved using the *hp*–adaptive version of the open-source pseudospectral optimal control software GPOPS[10–12] with the MATLAB version of the NLP solver SNOPT.[17]

IV. Initial Guess Generation Using RRT Algorithm

In order to solve the optimal control problem posed in Section III, it is necessary to supply initial guesses to the optimal control software. Rather than starting from naive initial guesses, the initial guesses for the optimal control software are obtained using a modification of a rapidly exploring random tree (RRT) path planning algorithm.[9] Specifically, we employ an RRT algorithm that consists of multiple trees that grow simultaneously toward a goal point similar to the work of Ref. 18. We attempt to connect these trees at each iteration, ultimately reaching the goal point in as short a time as possible. In order to avoid obstacles, the multiple RRT algorithm is modified such that the aircraft landing trajectories are determined in an order from closest to furthest in distance from the runway. The RRT algorithm takes the following inputs: (1) the total number of aircraft; (2) the initial position of each aircraft; (3) the position of the runway; and (4) the constraints on the (x, y, h) airspace. First, the aircraft and sorted in ascending distance order from the runway. The shortest path for each aircraft between the initial conditions and the landing point is determined that avoids the obstacle. In order to account for the time spacing between aircraft landings, all but the first aircraft are forced to reach the runway via a waypoint, where the waypoint is selected randomly to satisfy the time-spacing constraint. The waypoint is selected randomly from a constrained airspace $y > y_0$. The RRT algorithm is called repeatedly to find the total distance from the initial point to the goal point via the currently chosen way point. The waypoint is selected if the total distance traveled by aircraft to reach the goal point maintains a minimum and maximum distance of separation between two successive aircraft landings. Using the assumption of constant aircraft speed, the separation in distance translates into the time-spacing constraint for the optimal control problem. In order to avoid choosing a previously chosen waypoint on a future iteration, the previously chosen waypoints are stored in an array and are checked against the newly generated waypoints, The final landing times obtained using this approach are then used as part of the initial guess for the optimal control problem.

V. Results

The multiple aircraft optimal problem described in Section III was solved using the open-source program *General Pseudospectral Optimal Control Software*[10–12] (GPOPS) with the the initial conditions given in Table 1a, an initial time $t_0 = 0$, and the following values for the parameters: $A = (2, 3, 4)$, $T = 15$ s, $V = 80$ m/s, $\ell = 500$ m, and $c = 1/2$. In addition, the following limits were placed on the components of the state, control, and bank angle: $(x_{\max}, y_{\min}, y_{\max}, h_{\max}) = (6, 0, 12, 0.6)$ km, $(\gamma_{\max}, \phi_{\max}) = (90, 180)$ deg, $n_{\max} = 10$, and $\sigma_{\max} = 45$ deg. Next, the wall obstacle was constructed using the parameters given in Table 1b, while the parameters that specify the size of the opening that an aircraft must pass through at times $t_j^o,\ j = 1, \ldots, A$, are $(x_{\max}^o, h_{\min}^o, h_{\max}^o, y^o) = (2, 0.2, 0.4, 6)$ km, while the event constraint on the heading angle $\phi^o = -90$ deg. In addition, the terminal conditions, which corresponds to a south-facing runway, are given as $(x_f, y_f, h_f) = (0, 0, 0)$ km and $(\gamma_f, \phi_f) = (0, -90)$ deg. Finally, in the results that follow, the notation A_i denotes aircraft $i \in [1, \ldots, A]$.

The optimal trajectories for $A = (2, 3, 4)$ are shown in Figs. 1a–1c. It is seen that each aircraft is steered from its initial position to a position, $(x(t_j^o), y(t_j^o), h(t_j^o)),\ j = 1, \ldots, A$, at the opening in the obstacle such that the aircraft is closely aligned with the runway at the point where the aircraft passes through the opening. Furthermore, it is interesting to see that $h(t_j^o),\ j = 1, \ldots, A$ is only slightly larger that the lower limit than $h_{\min}^o$. The fact that $h(t_j^o),\ j = 1, \ldots, A$ is near its lower bound is consistent with the cost functional of Eq. (7) in that the first term of Eq. (7) attempts to maximize the time taken for the nearest aircraft to pass through the opening in the obstacle. Because the landing time of each aircraft is fixed, maximizing $t_j^o,\ j = 1, \ldots, A$ is equivalent to

Table 1: Initial State for Each Aircraft, Parameters for Wall Obstacle, Initial Guesses of Landing Times, and Optimal Landing Times.

(a) Components of Initial State of Each Aircraft.

Aircraft	x_0 (km)	y_0 (km)	h_0 (km)	γ_0 (deg)	ϕ_0 (deg)
A_1	2.4	11.6	0.56	0	-15
A_2	-3.6	12	0.5	0	-10
A_3	6	11	0.44	0	-105
A_4	-5.5	11.8	0.6	-2	-25

(b) Parameters for Wall Obstacle.

Obstacle k	y^o (km)	x_{ck} (km)	h_{ck} (km)	p	a_k (km)	c_k (km)	d_k (km)
1	6	-4	0.3	50	2	0.3	1
2	6	4	0.3	50	2	0.3	1
3	6	0	0.5	50	2	0.5	1
4	6	0	0.1	50	2	0.1	1

(c) Initial Guesses of Terminal Times, $t_{fj}^{\text{guess}},\ j = 1,\ldots,A$, Generated Using RRT Algorithm Alongside Optimal Terminal Times, $t_{fj}^{*},\ j = 1,\ldots,A$, and Optimal Times to Pass Through Opening in Obstacle, $t_j^{o^*},\ j = 1,\ldots,A$.

Case	Aircraft	t_{fj}^{guess}	t_{fj}^{*}	$t_j^{o^*}$
$A = 2$	A_1	148.23	155	79.68
	A_2	165.04	170	94.96
$A = 3$	A_1	148.23	155	79.68
	A_2	164.44	170	94.96
	A_3	180.45	185	109.96
$A = 4$	A_1	148.23	160	84.94
	A_2	165.41	175	99.96
	A_3	180.84	190	114.95
	A_4	196.18	205	129.96

minimizing the time, $t_{fj} - t_j^o$, taken for an aircraft to land after passing through the opening in the obstacle. Minimizing $t_{fj} - t_j^o$ requires that the obstacle be as close to the runway as possible at the obstacle crossing point, thus requiring that $h(t_j^o),\ j = 1, \ldots, A$ be as low as possible.

Another interesting feature of the optimal trajectories is given in Figs. 2a–2c, where it is seen that each aircraft follows a nearly straight line trajectory from $t_j^o,\ j = 1, \ldots, A$, to $t_{fj},\ j = 1, \ldots, A$. In particular, it is noted that x is quite small during a phase after an aircraft has passed through the opening in the obstacle. The direct path taken by an aircraft after passing through the opening in the obstacle is consistent with the inclusion of the second term in the cost functional of Eq. (7) where effectively the amount of crossrange maneuvering is minimized over the entire trajectory.

Another important feature of the optimal trajectories is found in Fig 3a–3c which shows the flight path angle for $A = (2, 3, 4)$. Specifically, it is seen during the pre-obstacle phases of flight that γ remains largely negative, indicating that the direction of velocity remains largely below the horizontal direction. Due to the constraint that $\gamma(t_j^o) = 0$, however, the flight path angle increases temporarily at $t_j^o,\ j = 1, \ldots, A$, before decreasing during the post-obstacle phases of flight. If the constraint $\gamma(t_j^o) = 0$ were removed from the problem, the flight path angle would remain negative prior to meeting the terminal condition $\gamma(t_{fj}) = 0$.

Next, Figs. 4–6 show the bank angle for the different aircraft landing scenarios. It is interesting to notice a key differences in the behavior of the bank angle before and after an aircraft passes through the opening in the obstacle. During pre-obstacle flight, each aircraft performs a large crossrange maneuver in order to align itself with the runway. During post-obstacle flight, however, each aircraft performs a minimal amount of crossrange maneuvering because the alignment was done prior to passing through the opening in the obstacle. Moreover, it is interesting to see in Figs. 4–6 that the bank angle is continuous and smooth during all pre-obstacle phases. At the point where an aircraft passes through the opening in the obstacle, however, in all cases the bank angle changes discontinuously. The discontinuous change at the start of post-obstacle flight is again consistent with the design of the cost functional where it is desired to keep crossrange maneuvering to a minimum during post-obstacle flight. Specifically, it is seen that σ is small during post-obstacle flight, implying that the lift is oriented nearly vertically upward upon crossing the obstacle and, thus, lateral motion is largely suppressed.

Finally, Table 1c shows the optimal time of each aircraft to reach the obstacle wall along with the final trajectory time of each aircraft. It is seen that the RRT algorithm generates a guess of t_f that is between 5 s and 10 s shorter than the optimal landing time t_f^*. In addition, it is seen that times required for the first and second aircraft to pass through the opening in the obstacle are separated by approximately 5 s, while the times required for the second, third, and fourth aircraft to cross the obstacle are separated by approximately 15 s.

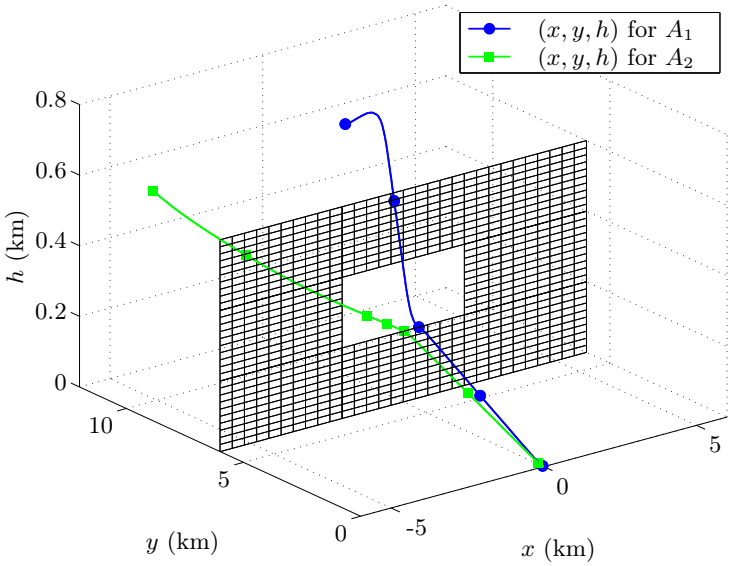

(a) Optimized Trajectories for $A = 2$.

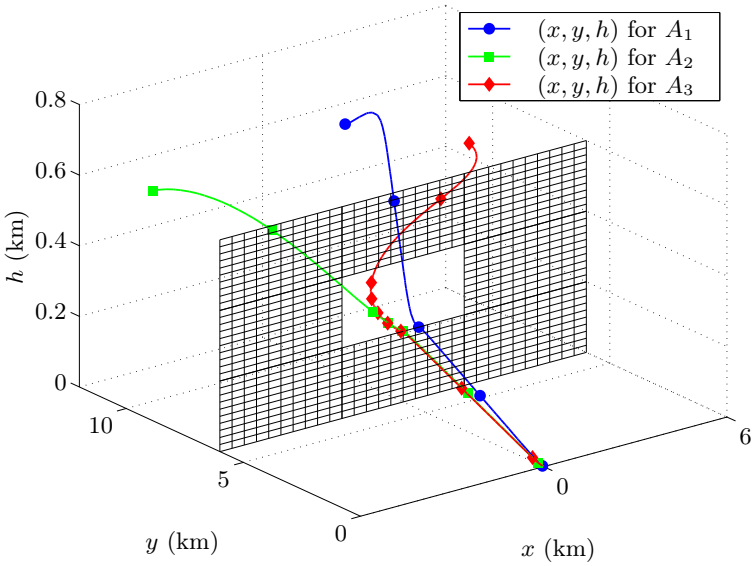

(b) Optimized Trajectories for $A = 3$.

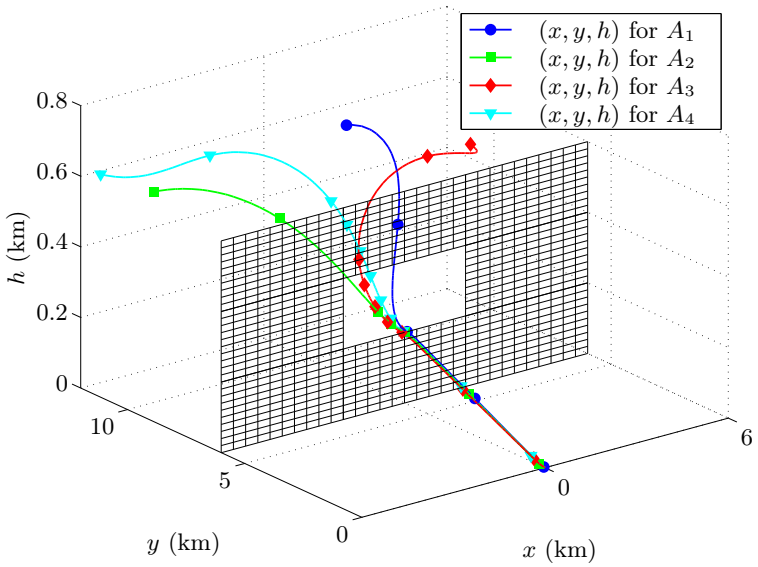

(c) Optimized Trajectories for $A = 4$.

Figure 1: Optimized Trajectories for $A = (2, 3, 4)$.

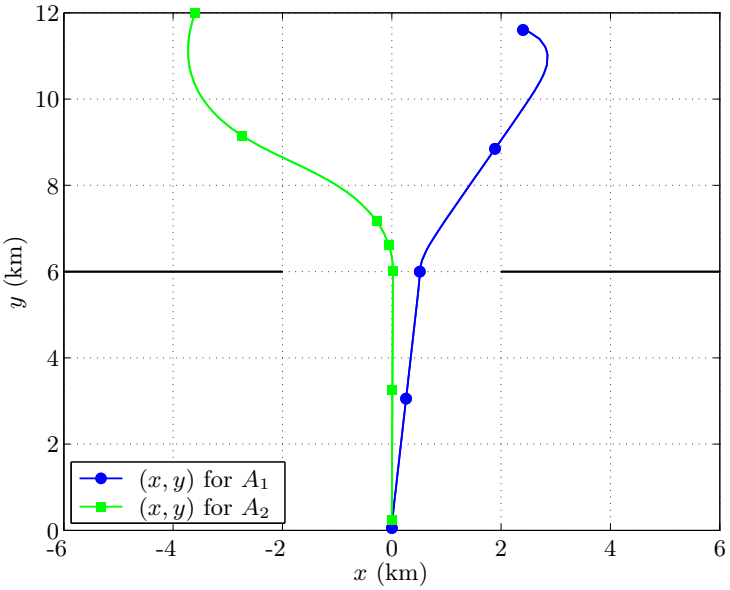

(a) (x, y)-Plane Projection of Optimal Trajectory for $A = 2$.

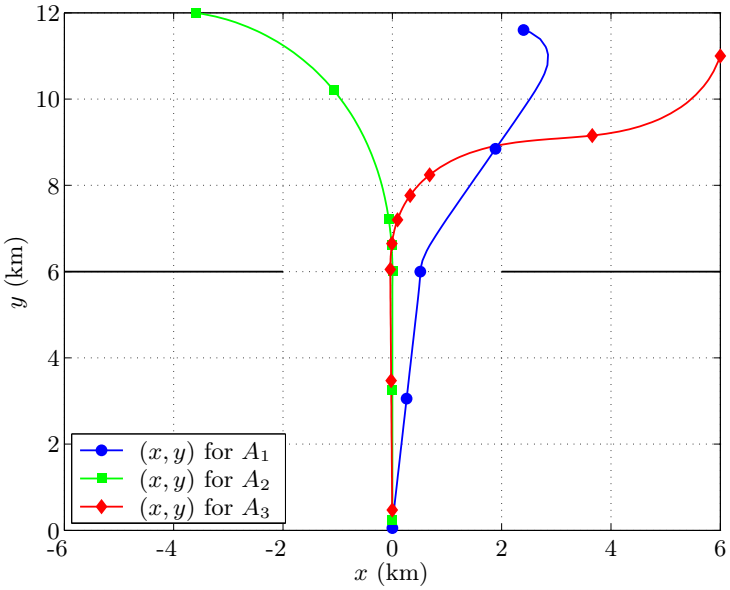

(b) (x, y)-Plane Projection of Optimal Trajectory for $A = 3$.

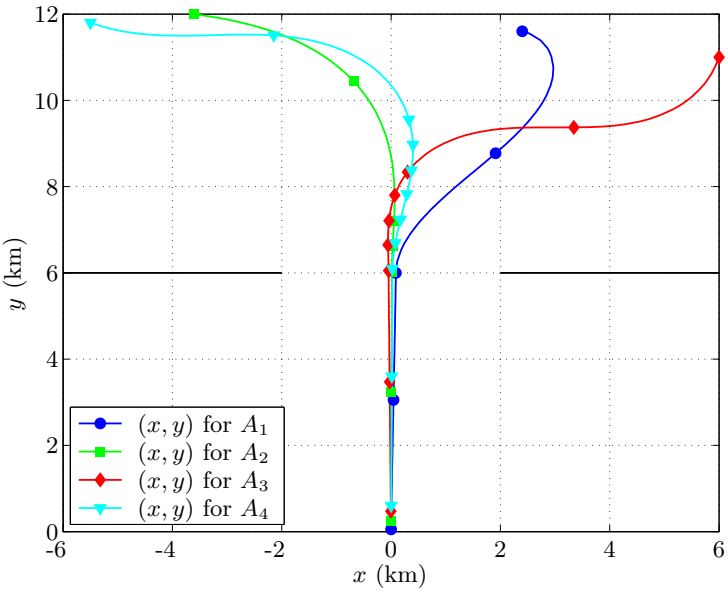

(c) (x, y)-Plane Projection of Optimal Trajectory for $A = 4$.

Figure 2: Projection of Optimized Trajectories Into the (x, y)-Plane for $A = (2, 3, 4)$.

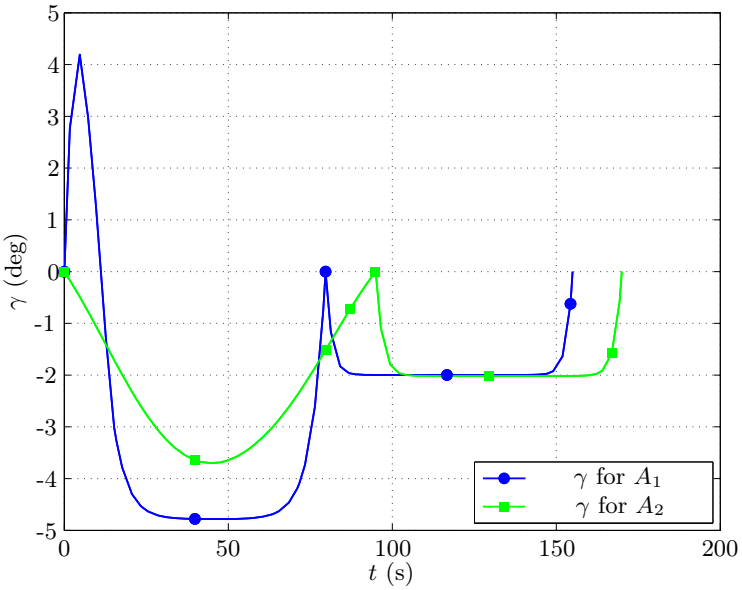

(a) A_1 and A_2 Flight Path Angle, γ, vs. Time, t, for $A = 2$.

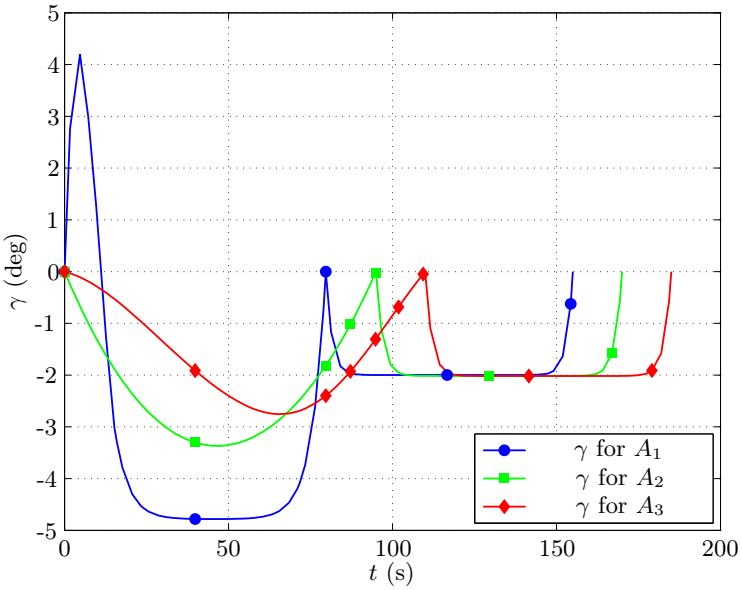

(b) A_1, A_2, and A_3 Flight Path Angle, γ, vs. Time, t, for $A = 3$.

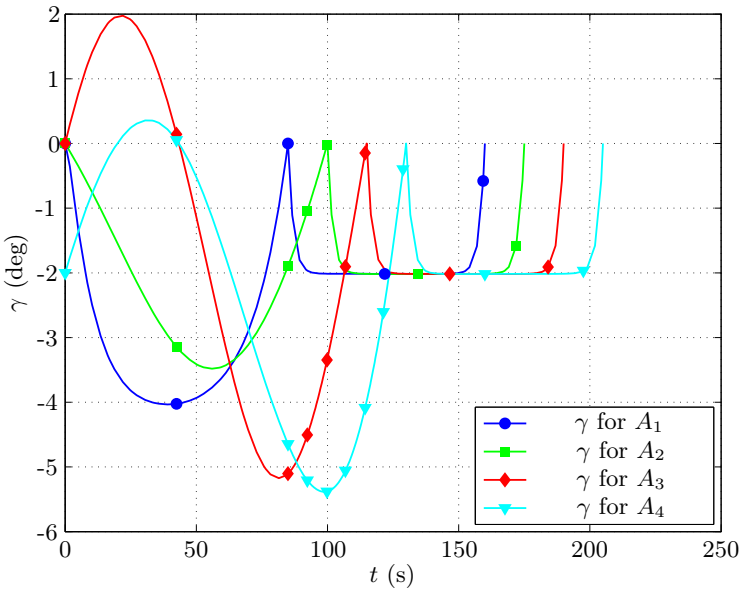

(c) A_1, A_2, A_3, and A_4 Flight Path Angle, γ, vs. Time, t, for $A = 4$.

Figure 3: Flight Path Angle, γ, vs. Time, t, for $A = (2, 3, 4)$.

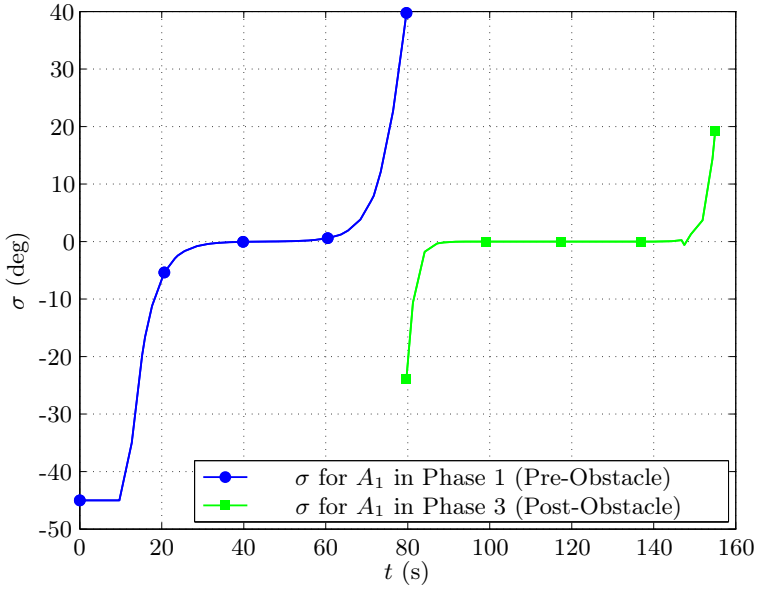

(a) A_1 Bank Angle, σ, vs. Time, t, for $A = 2$.

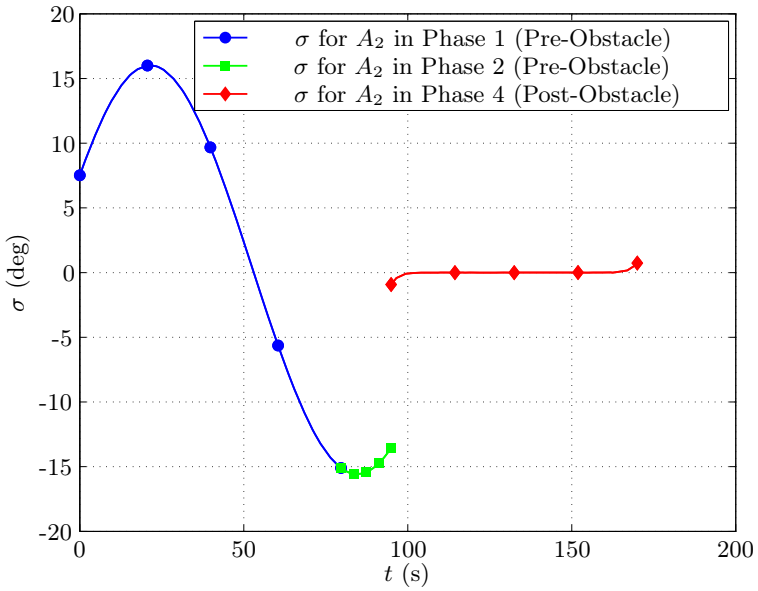

(b) A_2 Bank Angle, σ, vs. Time, t, for $A = 2$.

Figure 4: Bank Angle, σ, vs. t, for $A = 2$.

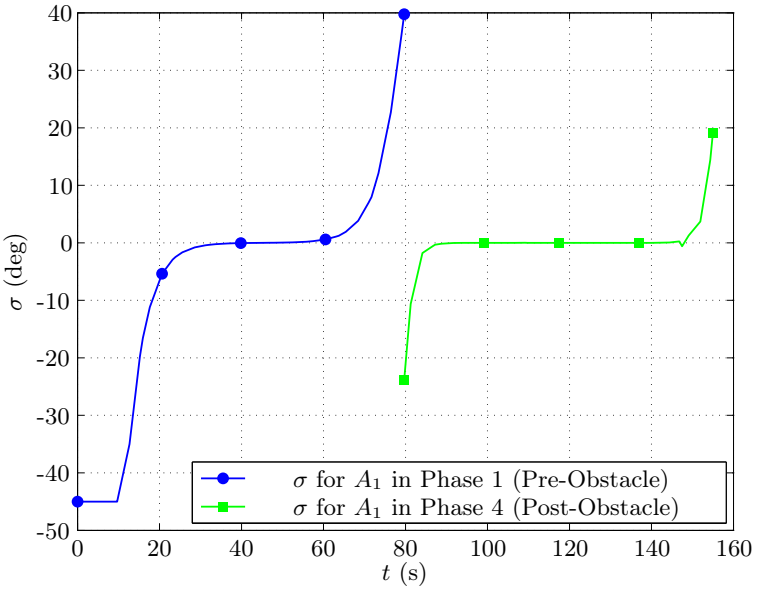

(a) A_1 Bank Angle, σ, vs. Time, t, for $A = 3$.

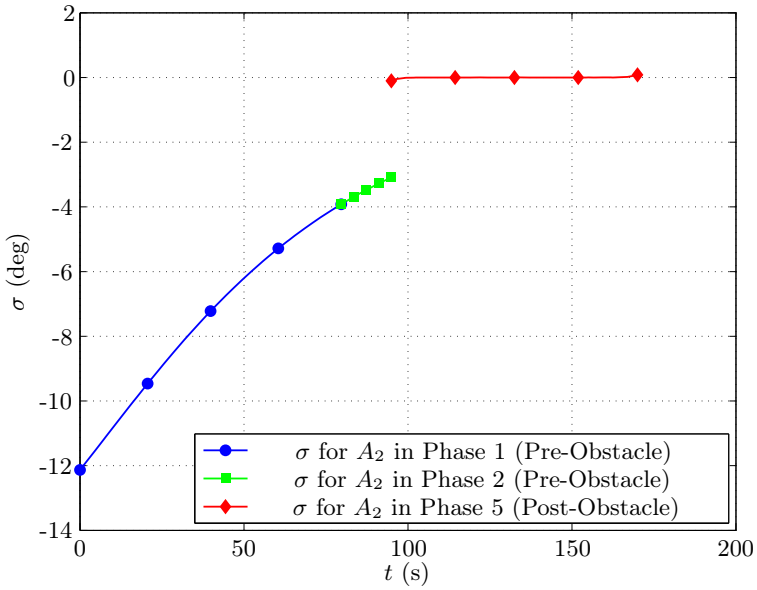

(b) A_2 Bank Angle, σ, vs. Time, t, for $A = 3$.

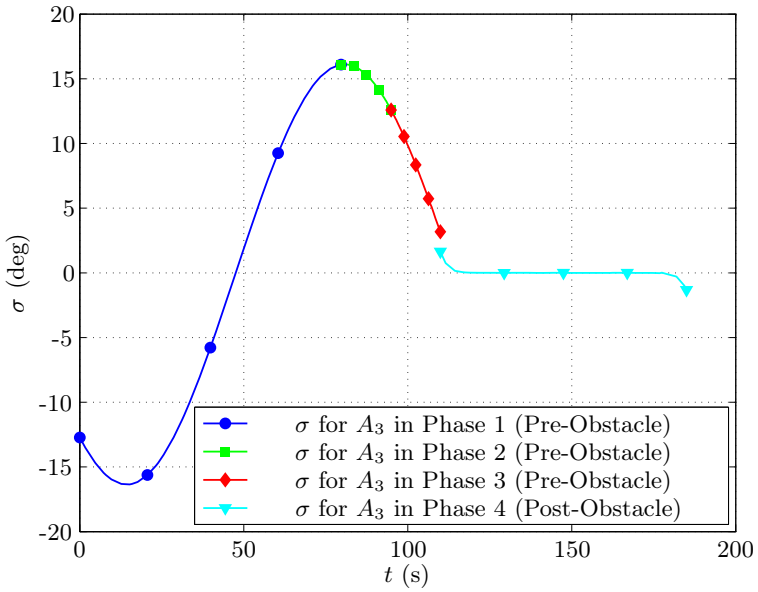

(c) A_3 Bank Angle, σ, vs. Time, t, for $A = 3$.

Figure 5: Bank Angle, σ, vs. t, for $A = 3$.

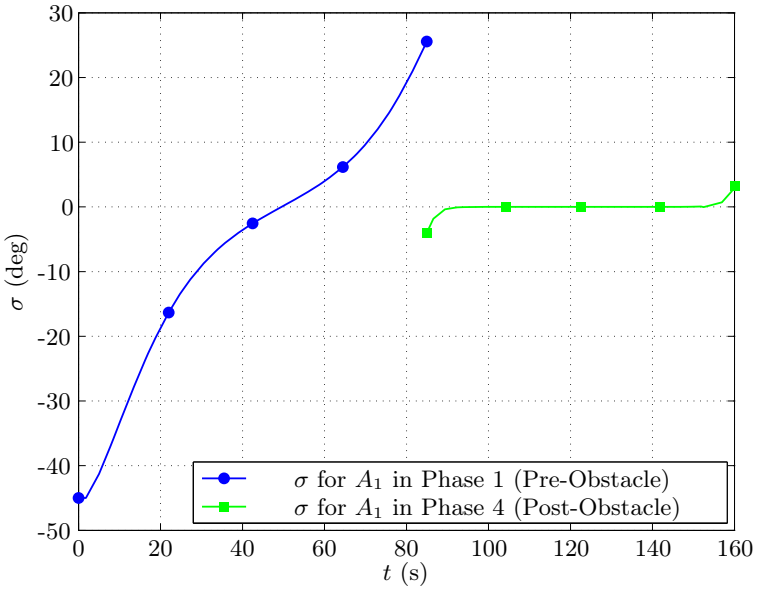

(a) A_1 Bank Angle, σ, vs. Time, t, for $A = 4$.

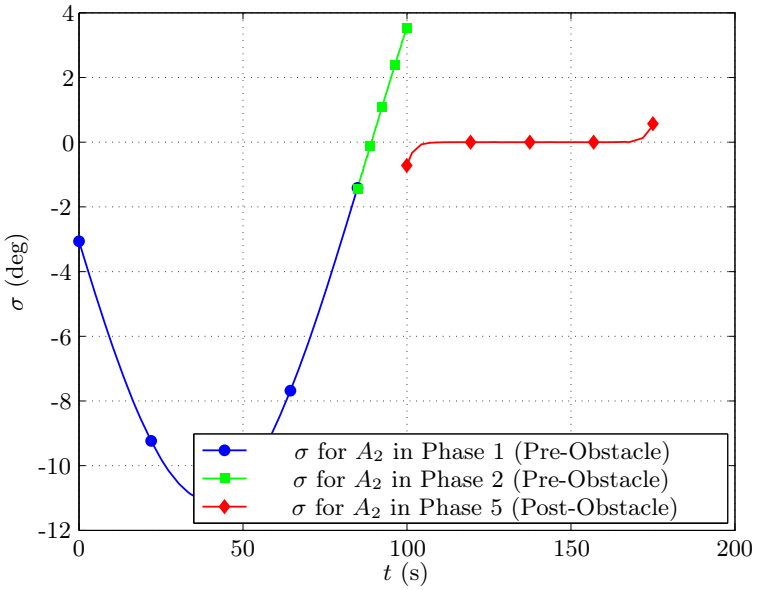

(b) A_2 Bank Angle, σ, vs. Time, t, for $A = 4$.

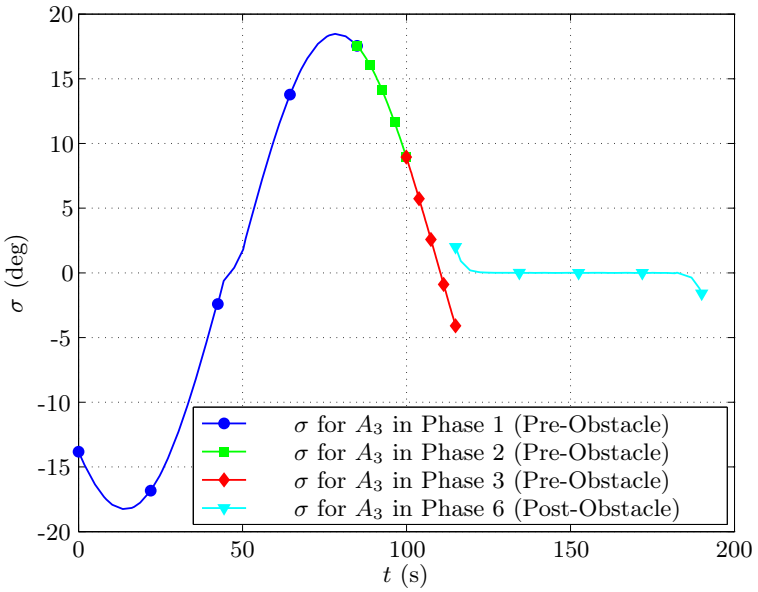

(c) A_3 Bank Angle, σ, vs. Time, t, for $A = 4$.

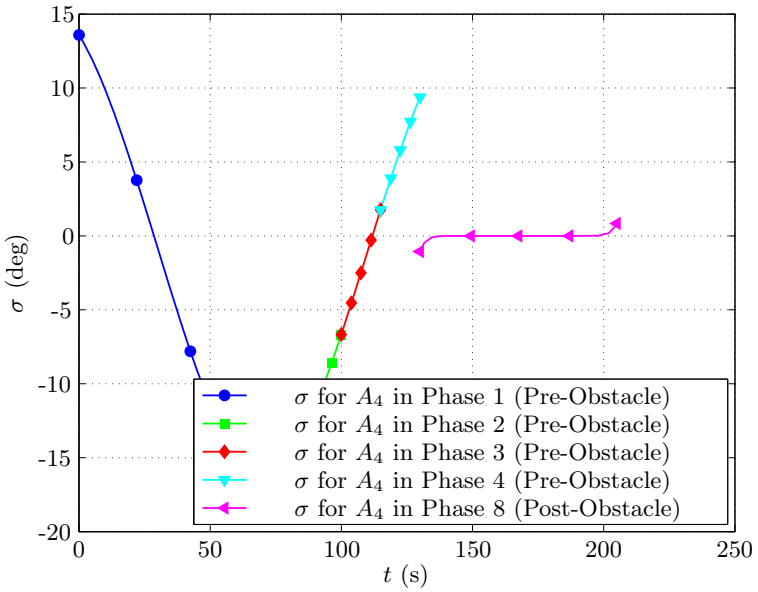

(d) A_4 Bank Angle, σ, vs. Time, t, for $A = 4$.

Figure 6: Bank Angle, σ, vs. t, for $A = 4$.

VI. Conclusions

A numerical optimization study of optimal landing of multiple aircraft on a single runway in the presence of an obstacle has been considered. Optimal trajectories were determined by solving a non-sequential constrained multiple-phase optimal control problem. The pre-obstacle phases consisted of the motion of multiple aircraft under a collision-avoidance constraint with a hybrid cost functional of maximizing the time to reach the obstacle and minimizing the crossrange maneuvering, while the post-obstacle phases consisted of a single aircraft with a cost functional of minimizing the crossrange maneuvering. The multiple-phase optimal control aircraft landing problem is solved using a previously developed open-source optimal control software and the key features of the optimal trajectories have been identified. The approach used in this paper is found to be viable for generating optimal trajectories and controls for multiple-aircraft landing.

Acknowledgments

The authors gratefully acknowledge support for this research by the U.S. Office of Naval Research under Grant N00014-11-1-0068.

References

[1]Lecchini, A., Glover, W., Lygeros, J., and Maciejowski, J., "Air-Traffic Control in Approach Sectors: Simulation Examples and Optimisation," *Hybrid Systems: Computation and Control*, Springer Berlin / Heidelberg, 2005.

[2]Malaek, S. M. and Nabavi, S. Y., "Near-Optimal Trajectories to Manage Landing Sequence in the Vicinity of Controlled Aerodromes," *Journal of Aircraft*, Vol. 47, No. 1, JAN-FEB 2010, pp. 129–140.

[3]Brentnall, A. R. and Cheng, R. C. H., "Some effects of aircraft arrival sequence algorithms," *Journal of the Operational Research Society*, Vol. 60, No. 7, JUL 2009, pp. 962–972.

[4]Wickenheiser, A. M. and Garcia, E., "Optimization of perching maneuvers through vehicle morphing," *Journal of Guidance, Control, and Dynamics*, Vol. 31, No. 4, JUL-AUG 2008, pp. 815–823.

[5]Bauerle, N., Engelhardt-Funke, O., and Kolonko, M., "Routing of airplanes to two runways - Monotonicity of optimal controls," *Probability in the Engineering and Informational Sciences*, Vol. 18, No. 4, 2004, pp. 533–560.

[6]Menon, P. K., Sweriduk, G. D., and Sridhar, B., "Optimal Strategies for Free-Flight Air Traffic Conflict Resolution," *Journal of Guidance, Control, and Dynamics*, Vol. 22, No. 2, January 1999, pp. 202–212.

[7]Raghunathan, A. U., Gopal, V., Subramanian, D., Biegler, L. T., and Samad, T., "Dynamic Optimization Strategies for Three-Dimensional Conflict Resolution of Multiple Aircraft," *Journal of Guidance, Control, and Dynamics*, Vol. 27, No. 4, July-August 2004, pp. 586–594.

[8]Patel, R. B. and Goulart, P. J., "Trajectory Generation for Aircraft Avoidance Maneuvers Using Online Optimization," *Journal of Guidance, Control, and Dynamics*, Vol. 34, No. 1, January-February 2011, pp. 218–230.

[9]Lavalle, S. M., "Rapidly-Exploring Random Trees: A New Tool for Path Planning," 1999.

[10]Darby, C. L., Hager, W. W., and Rao, A. V., "Direct Trajectory Optimization Using a Variable Low-Order Adaptive Pseudospectral Method," *Journal of Spacecraft and Rockets*, Vol. 48, No. 3, May–June 2010, pp. 433–445.

[11]Darby, C. L., Hager, W. W., and Rao, A. V., "An hp-Adaptive Pseudospectral Method for Solving Optimal Control Problems," *Optimal Control Applications and Methods*, Vol. 32, No. 4, July–August 2010, pp. 476–502, DOI: 10.1002/oca.957.

[12]Rao, A. V., Benson, D. A., Darby, C. L., Francolin, C., Patterson, M. A., Sanders, I., and Huntington, G. T., "Algorithm 902: GPOPS, A Matlab Software for Solving Multiple-Phase Optimal Control Problems Using the Gauss Pseudospectral Method," *ACM Transactions on Mathematical Software*, Vol. 37, No. 2, April–June 2010, Article 22, 39 pages.

[13]Aoude, G. S., "Two-Stage Path Planning Approach for Solving Multiple Spacecraft Reconfiguration Maneuvers," *The Journal of the Astronautical Sciences*, Vol. 56, No. 4, September–December 2008, pp. 515–544.

[14]Benson, D. A., Huntington, G. T., Thorvaldsen, T. P., and Rao, A. V., "Direct Trajectory Optimization and Costate Estimation via an Orthogonal Collocation Method," *Journal of Guidance, Control, and Dynamics*, Vol. 29, No. 6, November-December 2006, pp. 1435–1440.

[15]Garg, D., Patterson, M., Hager, W. W., Rao, A. V., Benson, D. A., and Huntington, G. T., "A Unified

Framework for the Numerical Solution of Optimal Control Problems Using Pseudospectral Methods," *Automatica*, Vol. 46, No. 11, November 2010, pp. 1843–1851.

[16]Dai, R., *Three-Dimensional Trajectory Optimization in Constrained Airspace*, Ph.D. thesis, Auburn University, 2007.

[17]Gill, P. E., Murray, W., and Saunders, M. A., "SNOPT: An SQP Algorithm for Large-Scale Constrained Optimization," *SIAM Review*, Vol. 47, No. 1, January 2002, pp. 99–131.

[18]Clifton, M., Paul, G., Kwok, N., Liu, D., and Wang, D. L., "Evaluating Performance of Multiple RRTs," *Mechtronic and Embedded Systems and Applications, 2008. MESA 2008. IEEE/ASME International Conference on*, 2008, pp. 564–569.